Int. J. Multiphase Flow Vol. 16, No. 2, pp. 261–279, 1990
Printed in Great Britain.

0301-9322/90 \$3.00 + 0.00

THE DRIFT–FLUX MODEL APPLIED TO BUBBLE COLUMNS AND LOW VELOCITY FLOWS

N. N. Clark, J. W. Van Egmond and E. P. Nebiolo
Department of Mechanical & Aerospace Engineering, West Virginia University, Morgantown, WV 26506, U.S.A.

(*Received* 7 *October* 1988; *in revised form* 25 *September* 1989)

Abstract—Although the drift–flux model is well-established for use in high velocity bubble flows, many researchers have found the need to alter the model to deal with low velocities or large diameter pipes. Based on some preliminary bubble distribution data from a 15.2 cm dia bubble column and on data in the literature, a program has been written to establish values for the drift–flux profile constant C_0 when it is influenced by buoyancy effects. It is concluded that the drift–flux model must be used with caution since C_0 can vary from <1 to values >10 under extreme circumstances. However, C_0 is shown to assume the accepted values in higher velocity flows where buoyancy can be neglected. In addition, a technique is presented for predicting circulation in a column without prior knowledge of the void (bubble) distribution.

Key Words: two-phase flow, bubble column, drift–flux model circulation

INTRODUCTION

Prediction of the gas void fraction in upward gas–liquid flows has received much attention in the engineering literature over the past 20 years. Many studies of boiling flows were spurred by nuclear power plant development, while more recent work has arisen from a need to study air-lift loop reactors. Throughout this time analyses of vertical air-lift pumps have also appeared in the literature. Most widely used for void fraction prediction are drift–flux models, of the type proposed by Nicklin (1962) and by Zuber & Findlay (1964), which have been discussed in the subsequent literature (Nassos & Bankoff 1967; Clark & Flemmer 1984; Hills 1976). However, when the drift–flux model has been applied to very low velocity bubble flows and large diameter pipes, it is found that the "constants" in the model vary significantly. In addition, these constants have been shown experimentally to vary with void fraction at low velocity flows. This is not to say that the drift–flux model is incorrect in this case, but that the velocity and void fraction distributions vary widely under these circumstances and may be very sensitive to operating conditions. By adapting a force-balance model, usually used for tall bubble columns (where there is no liquid flow), to account for a small upflow or downflow, the authors have examined the effect of buoyancy on the drift–flux profile parameter C_0. Results show, as one might expect, that buoyancy effects may be significant in large diameter systems with low flowrates. This conclusion should be of interest to those designing biological loop reactors (Onken & Weiland 1983), deep shift reactors (Hines *et al.* 1975), Fischer–Tropsch bubble column reactors (Stern *et al.* 1985) and coal flotation columns (Im *et al.* 1987). In addition, this research has resulted in design diagrams for the prediction of bubble column holdup.

Literature Review: Drift–Flux Model

Zuber & Findlay (1964) have presented an exhaustive derivation for the drift–flux model, which is based on the argument that holdup in a two-phase flow (typically bubble, slug or churn gas–liquid flow) is influenced by two separate phenomena. Firstly, it is acknowledged that the gas rises locally relative to the liquid due to phase density differences, a fact which may often be neglected in high velocity flows. Secondly, where a velocity distribution exists in the pipe, and where the gas is inhomogenously distributed across the pipe diameter, the gas may concentrate in a faster or slower region of flow, thus affecting the average gas holdup. The model is usually presented in the form

$$\frac{\bar{W}_G}{\bar{\epsilon}} = C_0(\overline{W_G + W_L}) + \frac{\overline{U_{Gm}\epsilon}}{\bar{\epsilon}},$$

Table 1. Values determined for C_0 in churn–turbulent bubble flow

Author(s)	Comment	Value of C_0
Wallis (1969)	Recommendation	1.2
Govier & Aziz (1972)	Recommendation	1.2–1.3
Ishii & Grolmes (1978)	Recommendation	$1.2–0.2\ (\rho_G/\rho_L)^{0.5}$
Nassos & Bankoff (1967)	69 mm pipe	1.1
Best fit/data of Borishanskiy *et al.* (1977)	11 mm pipe	1.187
Hewitt (1977)	Recommendation	1.2
Zuber & Findlay (1964)	50 mm pipe (includes slug flow)	1.2
Zuber *et al.* (1967)	Recommendation	1.2–1.3
Galaup (1975)	42 mm pipe	1.13
Clark & Flemmer (1984)	50 mm pipe	1.16

where W_G is the gas volumetric flux (superficial velocity), W_L is the liquid volumetric flux, ϵ is the void fraction, U_{Gm} is the relative velocity between the gas and the *mixture* [i.e. $U_{Gm} = U_G - (W_G + W_L)$, where U_G is the gas velocity] and an overbar denotes an average over the column cross section. The profile constant C_0 is given by

$$C_0 = \frac{\overline{\epsilon\,(W_G + W_L)}}{\bar{\epsilon}\,\overline{(W_G + W_L)}}$$

and is a measure of the interaction of the void and velocity distributions. Where the gas is more concentrated in the faster region of flow, $C_0 > 1$, and C_0 is often taken as 1.2 for fast upward bubble flows, as shown in table 1 above.

The term $\overline{U_{Gm}\epsilon}/\bar{\epsilon}$ is the weighted average drift velocity, accounting for the local slip. Since it has been shown that the relative (bubble rise) velocity U_{GL} $(= U_G - U_L)$ varies little over the pipe diameter (Serizawa *et al.* 1975), and since $U_{Gm} = U_{GL}\ (1 - \epsilon)$, with $\epsilon < 0.25$ in bubble flow, the weighted average drift velocity is often taken as the rise velocity of a bubble in an infinite medium, U_∞. Experimental data generally support this simplification.

The drift–flux model has not remained inviolate. There is a mounting body of data to show that either C_0 or $\overline{U_{Gm}\epsilon}/\bar{\epsilon}$ cannot be taken as constant over an operating range. For example, Hills (1976), using a 0.15 m pipe, acquired data which led to the development of a modified drift–flux model. Also Shipley (1984), working with a "toy tower" circulation loop of 0.457 m dia, found his data best correlated by the dimensional equation

$$\frac{\bar{W}_G}{\bar{\epsilon}} = 1.2\,(\bar{W}_G + \bar{W}_L) + 0.24\left(\frac{\text{m}}{\text{s}}\right) + 0.35\left(\frac{\bar{W}_G}{\bar{W}_G + \bar{W}_L}\right)^2 (gD\bar{\epsilon})^{1/2},$$

and some physical argument was provided for this approach. Clark & Flemmer (1985), using a 100 mm dia forced circulation loop in bubble flow, preferred to vary C_0 as a function of void fraction, since C_0 was found to be near 0.95 at low void fractions and near 1.2 when $\epsilon \approx 0.2$. Subsequently, Clark & Flemmer (1986) fitted the same data to a drift–flux model with two profile constants:

$$\frac{\bar{W}_G}{\bar{\epsilon}} = C_G\,\bar{W}_G + C_L\,\bar{W}_L + \frac{\overline{U_{Gm}\epsilon}}{\bar{\epsilon}},$$

with $C_G = 1.95$ and $C_L = 0.93$. Jones (1985) acquired data in a bubble column with draft tubes ranging from 44 to 146 mm dia. A drift–flux model overestimated the circulation in this column rate unless C_0 was set to very high values (2 to 5) (Clark & Jones 1987). Further argument on the variation of C_0 has been presented by Lorenzi & Sotgia (1978), while careful consideration of the definition of C_0 in the light of experimentally measured void and velocity profiles presented by Galaup (1975) and Serizawa *et al.* (1975) also supports the argument that C_0 cannot remain constant.

Discussion of the Limiting Case: Bubble Columns

The bubble column represents the extreme case of bubble flow where net liquid velocity is zero and the gas simply bubbles up through the liquid. Generally, buoyancy effects and gas maldistribution cause circulation of liquid in the column. Even when gas is evenly distributed over the column base, circulation can occur, and it is worth taking the time to consider the mechanism governing circulation startup, since this has not been discussed elsewhere.

Let us assume that a column with even gas distribution starts to operate in an "ideal" or one-dimensional mode, where the gas void distribution is even over the cross section at all heights in the column, so that the mixture is homogenous and has the same density throughout the column. At this stage no gross liquid circulation would occur. Since most two-phase systems involve some degree of turbulence or mixing, let us propose that at some time a few bubbles move toward the center of the column, at any height, so that the concentration of bubbles is suddenly slightly higher near the center. Consider the mechanistic sequence of events which may arise. The mean mixture density in the central region of the column is now lower than the density in the outer annulus, so that the hydrostatic head is greater over the height of the annulus than over the same height of the central core. Both the annular and central regions have the same pressure at the liquid surface, so that the difference in the hydrostatic heads causes a radial pressure difference deeper in the column (in fact, at every height below the point where the bubbles moved inward initially). This, in turn, causes an inward radial movement of liquid and initiates liquid circulation.

Bubbles rising from the distributor plate in the annular region are now moved inward a little by this radial inward liquid movement: the result is that bubble concentration near the center of the column increases and the liquid circulation increases. There is a positive feedback between the circulation and the radial bubble movement. Rapidly a stronger circulation pattern develops and the radial inward currents above the distributor plate continue to sweep more of the bubbles toward the center of the column (by analogy this is an inverted classifier).

One might expect that the circulation pattern would continue to increase indefinitely, but increasing upward velocity in the central region reduces bubble holdup in that region and hence the difference in the hydrostatic heads tends to some limit. The driving force arising from the difference in heads is consumed by dissipation in the fluid (energy balance) or shear at the column walls (momentum balance).

The argument may also start by assuming that a small number of bubbles move initially into the annular region, in which case the inverse pattern is set up. Such patterns have been known to occur, especially in fluidized beds (Surma 1985; Lin *et al.* 1985). In fact, this argument could be applied to any pattern, even multiple patterns in large tanks (Otero *et al.* 1985). However, it would seem that in the case of bubble columns and fluidized beds there are some non-stochastic grounds for the selection of a specific pattern by initial bubble movement, because at high gas velocities the circulation pattern is always upward at the center: transition patterns have also been observed (Lin *et al.* 1985). This is discussed in more detail, and preliminary data are provided, at the end of this paper.

EXPERIMENTAL WORK ON BUBBLE COLUMN CIRCULATION

Although some excellent data due to Hills (1974) are available for the estimation of void fraction in a 15.2 cm dia bubble column, some preliminary work was undertaken to reaffirm the bubble distribution in another 15.2 cm dia column, shown in figure 1. This column was 45.7 cm high and was provided with 4 ports for probe access at 4 different heights in the column. Air was introduced into the liquid in the column by means of a plenum chamber and distributor arrangement. Distributor plates were readily interchangeable. Three types of distributor plates, similar to those used by Hills (1974), as illustrated in figures 2(a–c) were used to introduce the air. The flowrate of air was monitored with a rotameter. Further work has been undertaken in a tall 20.3 cm dia column of similar construction.

Resistance probes were used in the mixture of air and conducting liquid (water) to determine whether at any instant in time gas or liquid was present at a point in the mixture. Each probe consisted of a thin stainless steel tube carrying an insulated wire which was connected to a needle, insulated except at its tip and protruding from the end of the tube. The stainless steel tube was invariably in contact with the liquid along much of its length, while the small exposed tip was in contact with whatever phase was present at its location at any given time. Thus, when the probe tip was in liquid, the resistance measured between the tip and the stainless steel sheath was low,

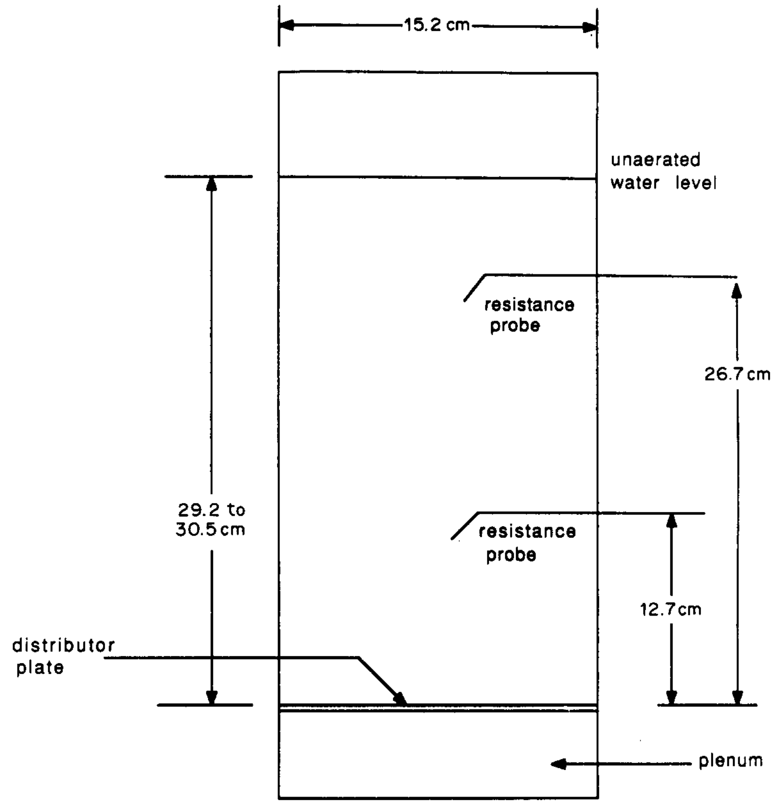

Figure 1. The 15.2 cm dia bubble column used to acquire void profiles.

but when the tip was surrounded by a bubble, the resistance was high. The probes used in the present research had the needle set into the end of the stainless steel tube with epoxy. For insulation, the protruding needle was then painted and the tip was lightly sanded to provide a very small sensing area. The probe tip was bent downwards so that it would pierce a rising bubble.

The resistance probes were incorporated in a resistance bridge circuit. This circuit communicated with an analog-to-digital (A/D) convertor (both 5 and 70 kHz boards have been used) in a personal computer. The circuit was such that the A/D convertor received a d.c. voltage close to 0 V when the probe tip was in air and 3.0–3.5 V when it was in water. It is believed that this latter voltage varied somewhat due to electrochemical effects since a d.c. circuit was used. Some other researchers have elected to use a.c. to reduce such effects, but this did not appear necessary in this preliminary work.

Theory dictates that the response from such a probe should be a square wave, generated by the switching of phase at the probe tip. Experience has shown that the signal pulses corresponding to bubbles are not square, but rounded because of the finite tip size and the time taken for liquid films to drain from the tip and establish themselves on the tip. The result is that these probes invariably underestimate the void fraction. It is therefore necessary to select a "cutoff" voltage to decide whether the probe tip is in the gas or liquid phase at any instant in time. Previous workers have generally used a Schmitt trigger to perform this function, but in the present work it was implemented with software. A program was written to collect the voltage from the probe at a large number of discrete times (generally 1000). Each voltage was then examined to see whether a bubble or liquid was present at the probe at that time, and a time-averaged gas void fraction was computed. To establish a cutoff voltage, the probe was operated at a fixed point with constant two-phase flow conditions in the column. During a preliminary work the time-averaged void fraction was computed using cutoff voltages varying from 0 to 3 V and a voltage of 1.625 V was selected as the cutoff voltage in the preliminary research, since this lay on the "plateau" of a plot of measured void fraction vs cutoff voltage.

Subsequent analysis of high-speed traces of the probe voltage signal has demonstrated that this primitive thresholding is unsatisfactory. Also, a comparison of the increase in column height with

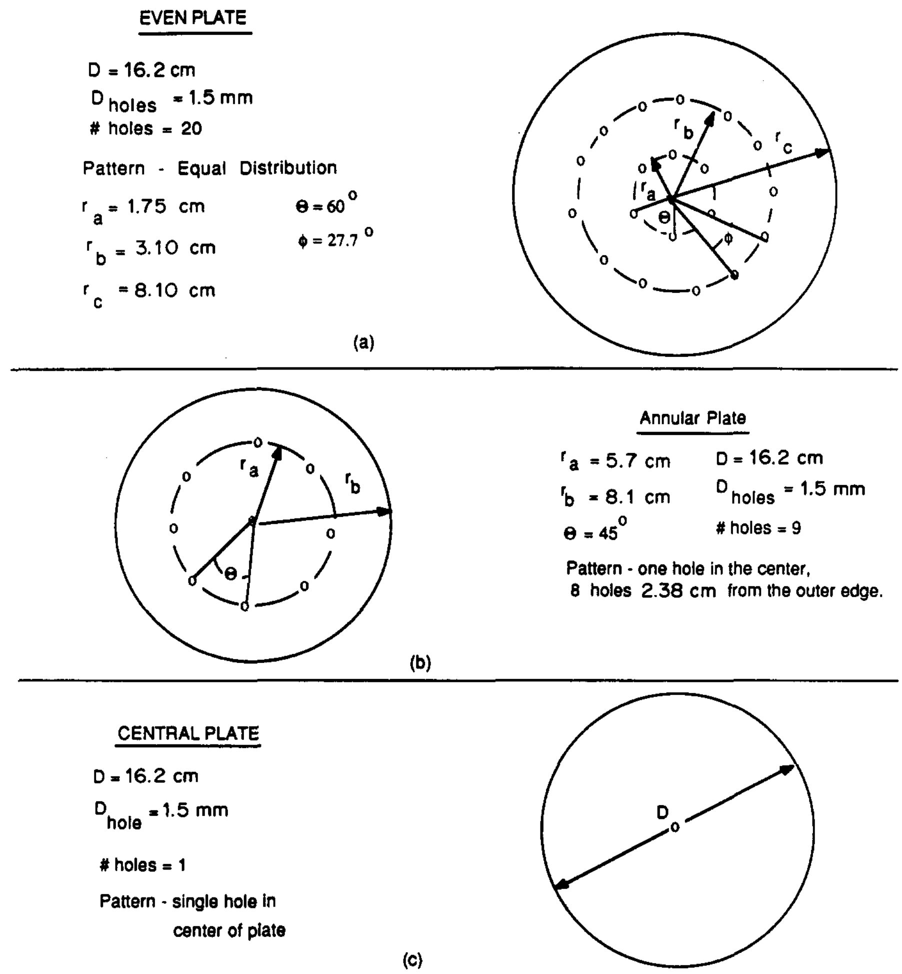

Figure 2. Distributor plates used in conjunction with the 15.2 cm dia column: (a) provides even air introduction; (b) provides central air introduction; (c) provides annular air introduction.

the local measured void fraction integrated throughout the column volume has shown that the probe with primitive thresholding may underestimate the void fraction by as much as 40%. The trace in figure 3, showing computer counts (proportional to voltage) vs time for a probe in the 20.3 cm dia column, demonstrates that the probe signal is certainly not a square wave. Brief intersections with bubbles lead to a small voltage drop, which may not be detected by the primitive thresholding, and more significant intersections still show a finite rate of voltage drop and rise. The authors have concluded from these traces and from cumulative frequency plots of measured voltage that a better threshold is a voltage which is very slightly lower than the typical voltage when the tip is in water. A final criterion chosen for the threshold was 0.025 V less than the voltage at the 50th percentile on the cumulative frequency plot of voltage, this percentile being an excellent estimate of the probe voltage in water. Since measured void fractions are always $<50\%$, this approach proves to be reliable and quite objective. The new thresholding criterion has led to an improvement in void fraction measurement: the void fraction measured by the probes is then $<10\%$ lower than the void fraction implied by column expansion.

Measured void distributions in the 15.2 cm dia column using primitive thresholding were generally high at the center and low at the walls, which is the expected distribution. Figures 4a and 4b show typical measured void profiles with an even gas distribution at the bottom of the column. Figure 5a shows the void distribution which results when gas is introduced through a single central orifice: a jet or train of bubbles is evident at the column center. Figure 5b shows the void distribution when air is introduced in an annular fashion at the distributor plate. Even though the local void fractions shown in figures 4a, b and 5a, b are lower than the true void fraction present,

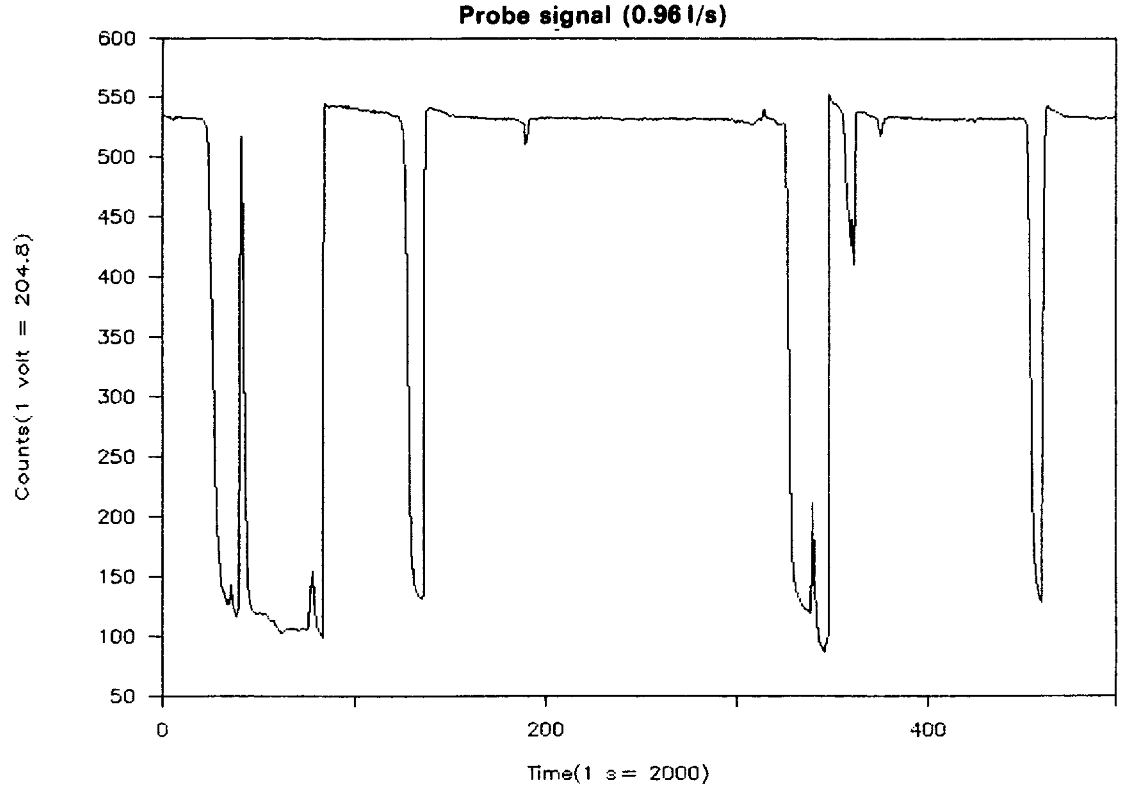

Figure 3. Trace of computer counts (proportional to voltage) vs time for a resistance probe in the 20.3 cm dia column. Primitive thresholding would determine the void fraction by using a cutoff of about 350 counts, leading to underestimation of the void fraction. A cutoff of 500 counts proves more accurate, though the void fraction is still slightly underestimated.

due to finite tip size, they show conclusively the variation of void fraction with radius. Based on these new data and the data of Hills (1974), the authors feel safe in approximating the void distribution by a radial power law expression, as presented in the analysis section below.

Figure 6 presents two traverses, generated using the improved thresholding, at right angles to one another, across the diameter of the 20.3 cm dia column at half the height of the mixture and at an air flowrate of approx. 94 l/s. Figure 6 shows that trends in void fraction determined with the improved thresholding also suggest that a radial power law model will be suitable.

PREDICTING C_0 IN CIRCULATING SYSTEMS

The model presented below considers a gas bubbled through a deep aspect ratio column, containing a liquid or non-setting slurry. This one-dimensional analysis considers only axial flows, and therefore is inapplicable to shallow aspect ratio columns. In bubble columns, circulating flows are generated by the variation of voidage, $\epsilon(r)$, and hence mixture density, with radial position, r.

As shown above, the voidage profile in bubble columns can be characterized by the following equation:

$$\epsilon(r) = \epsilon_c\left[1 - \left(\frac{r}{R}\right)^p\right], \quad [1]$$

where ϵ_c is the voidage at the center of the column and R is the radius of the column.

The density, $\rho(r)$, as a function of position is given then by

$$\rho(r) = \rho_L[1 - \epsilon(r)] + \rho_G\epsilon(r), \quad [2]$$

where ρ_L is the liquid density, and ρ_G, the gas density, is usually neglected. Substituting the

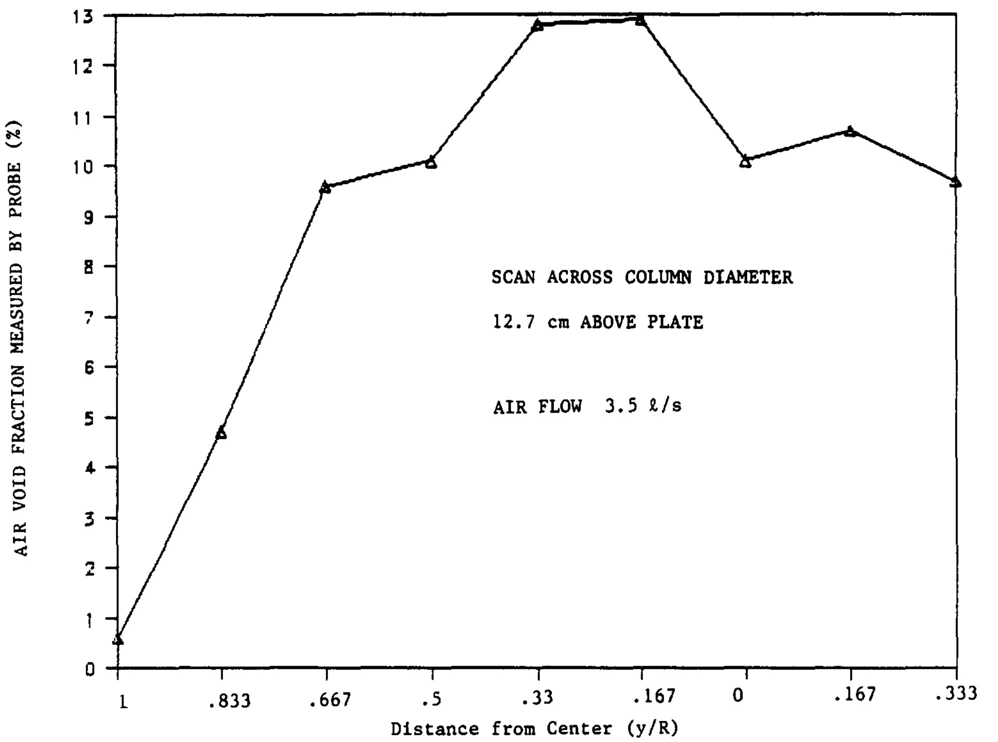

Figure 4a. Void profile measured across the column using a resistance probe, with the "even" plate illustrated in figure 2(a), at an air flowrate of 3.5 l/s.

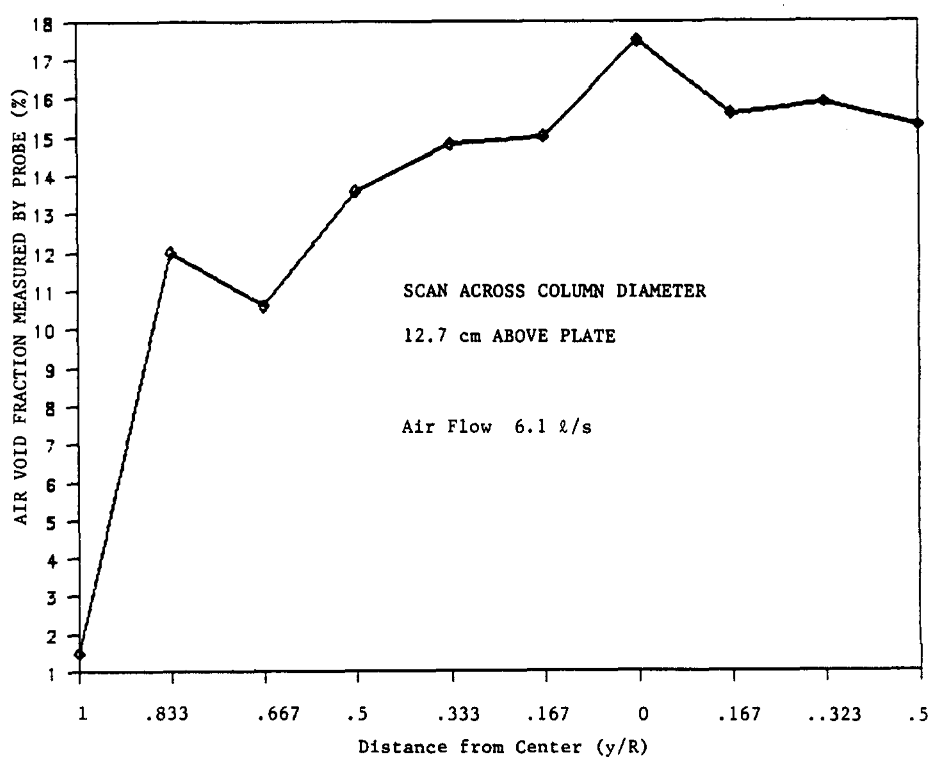

Figure 4b. Void profile measured across the column using a resistance probe, with the "even" plate illustrated in figure 2(a), at an air flowrate of 6.1 l/s.

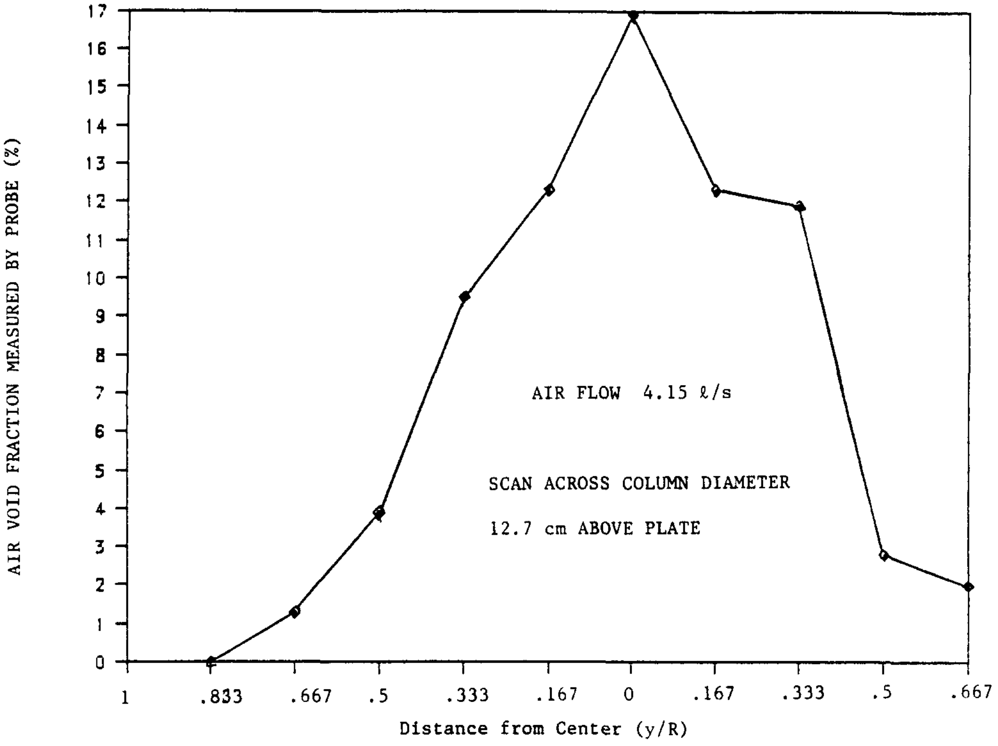

Figure 5a. Void profile measured across the column using a resistance probe, with the "central" plate illustrated in figure 2(b), at an air flowrate of 4.15 l/s. Central gas jetting is caused by this plate.

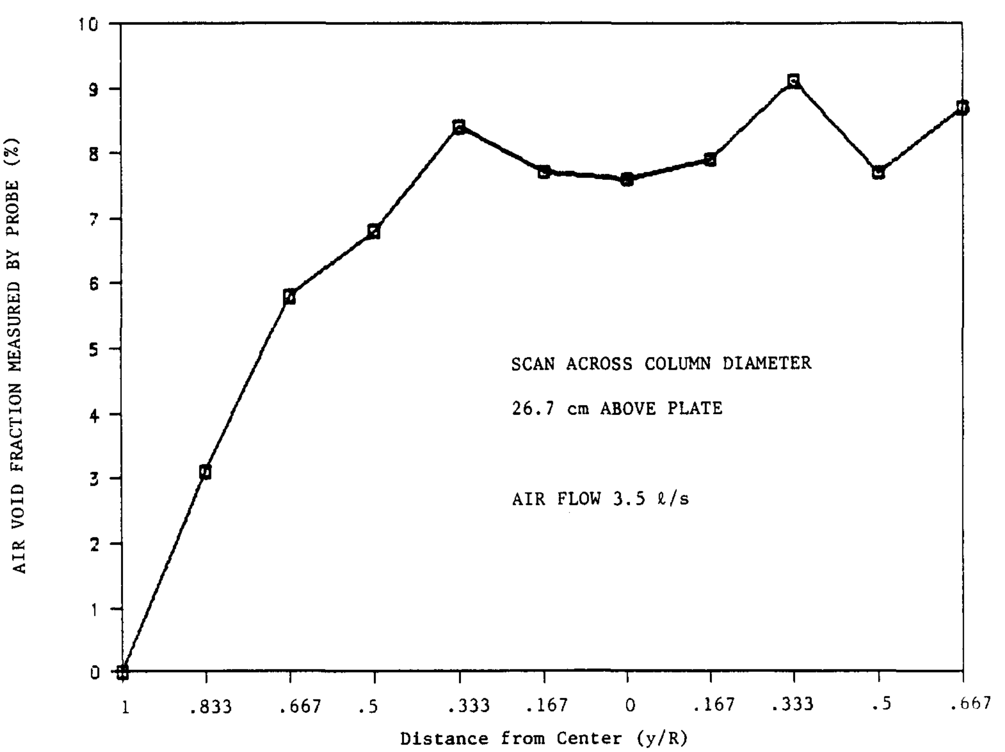

Figure 5b. Void profile measured across the column using a resistance probe, with the "annular" plate illustrated in figure 2(c), at an air flowrate of 3.5 l/s. The resulting gas distribution is more even than with the other two plates.

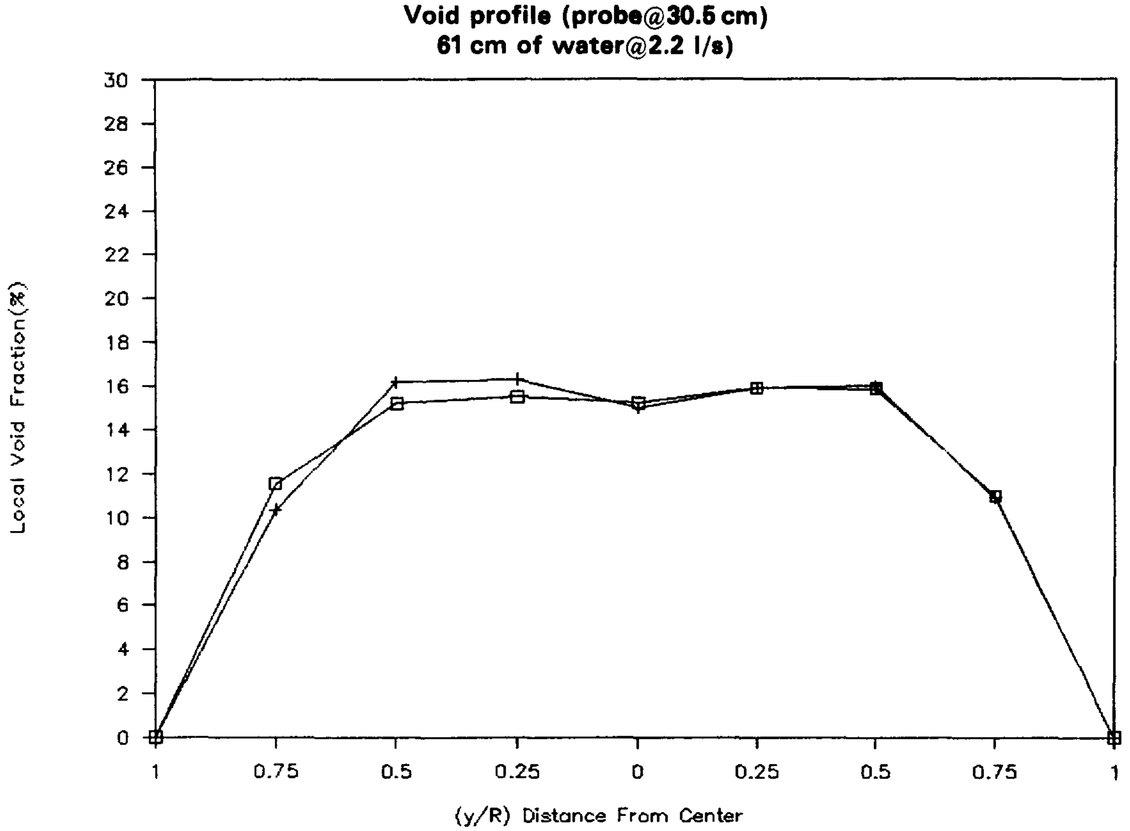

Figure 6. Void fraction variation across the diameter of the 20.3 cm dia column using improved thresholding. The two curves represent traverses at right angles to one another, and show that approximation by a radial power law should be satisfactory.

relationship for voidage into [2],

$$\rho(r) = \rho_L\left[1 - \epsilon_c + \epsilon_c\left(\frac{r}{R}\right)^p\right], \qquad [3]$$

the axial shear stress, $\tau(r)$, may be found (Clark *et al.* 1987; Levy 1963) using a force balance:

$$\tau(r) = \tau_w\left(\frac{r}{R}\right) + \frac{1}{2}rg[\bar{\rho} - \rho_i(r)], \qquad [4]$$

where g is gravitational acceleration and τ_w is the unknown wall shear stress. $\bar{\rho} - \rho_i(r)$ is the difference between the average density over the whole radius, and the average density within a radius, r, given by

$$\bar{\rho} - \rho_i(r) = \rho_L\left(\frac{2\epsilon_c}{\rho + 2}\right)\left[1 - \left(\frac{r}{R}\right)^p\right]. \qquad [5]$$

For the fluid in the column, a rheological mixing length model which takes into account turbulent momentum transfer, has found good agreement with data for turbulent water circulation, as shown by Clark *et al.* (1987). The shear stress was accordingly taken as

$$\tau(r) = \mu\left(\frac{dU}{dr}\right) + l^2\rho\left|\frac{dU}{dr}\right|\left(\frac{dU}{dr}\right), \qquad [6]$$

where μ is the viscosity, and l is the mixing length used by Clark *et al.* (1987):

$$\frac{l}{R} = 0.14 - 0.08\left(\frac{r}{R}\right)^2 - 0.06\left(\frac{r}{R}\right)^4. \qquad [7]$$

Those who choose to dispute [7] may observe that no better formulation exists, and that this has been used successfully before. The liquid velocity profile, $U(r)$, may be solved by equating shear stress in [4] and [6]:

$$0 = \tau_w\left(\frac{r}{R}\right) + \frac{rg}{2}(\bar{\rho} - \rho_i) - \mu\frac{\mathrm{d}u}{\mathrm{d}r} - l^2\rho\left|\frac{\mathrm{d}u}{\mathrm{d}r}\right|\left(\frac{\mathrm{d}u}{\mathrm{d}r}\right). \quad [8]$$

Using an assumed wall shear stress, $\mathrm{d}u/\mathrm{d}r$ was then found from [8] by using a Newton–Raphson method. Integrating from the wall boundary condition, $U = 0$ at $r = R$, the velocity $U(r)$ can then be found. Integrating $U(r)\,(1-\epsilon)$ over the column cross section then yields the liquid flux, $\bar{W}_L$:

$$\bar{W}_L = \frac{2}{R^2}\int_0^R U(r)\,(1-\epsilon)\,r\,\mathrm{d}r. \quad [9]$$

If W_L is equal to the desired liquid flux, then the assumed τ_w was correct. For example, if no net liquid flow is desired (bubble column), τ_w would have to be chosen until the integral in [9] assumed a value of zero. For the purpose of lucidity and efficiency, [8] may be made dimensionless, as follows:

$$0 = \left[N_{\tau_w} + \frac{\mathrm{Ga}}{2}\frac{\epsilon}{p+2}\right]r' - 2\frac{\mathrm{d}u'}{\mathrm{d}r'} - \left(\frac{l}{R}\right)^2(1-\epsilon)\mathrm{Ga}\left(\frac{\mathrm{d}u'}{\mathrm{d}r'}\right)\left|\frac{\mathrm{d}u'}{\mathrm{d}r'}\right|, \quad [10]$$

where

$$N_{\tau_w} = \frac{\tau_w}{\mu}\sqrt{\frac{D}{g}}, \quad [11]$$

$$u' = \frac{U}{\sqrt{gD}}, \quad [12]$$

$$r' = \frac{r}{R} \quad [13]$$

and

$$\mathrm{Ga} = \frac{\sqrt{gD}\,D\rho_L}{\mu}; \quad [14]$$

which is a Galileo number; D is the column diameter. Equation [9] may be rearranged to give:

$$\frac{\bar{W}_L}{\sqrt{gD}} = 2\int_0^1 u'(1-\epsilon)\,r'\,\mathrm{d}r'. \quad [15]$$

In order to determine the drift–flux parameter, C_0, it is necessary to find the average flux of the gas, W_G. The gas volume flux is given by

$$W_G = \epsilon\,U + \frac{\epsilon}{1-\epsilon}V_V. \quad [16]$$

Hence

$$W_G + W_L = U + \frac{\epsilon}{1-\epsilon}V_V; \quad [17]$$

and by definition,

$$C_0 = \frac{\int_0^R\left[\epsilon U + \frac{\epsilon^2}{1-\epsilon}V_V\right]r\,\mathrm{d}r}{\epsilon_c\left(1 - \frac{2}{p+2}\right)\int_0^R\left[U + \frac{\epsilon}{1-\epsilon}V_V\right]r\,\mathrm{d}r} \quad [18]$$

or

$$C_0 = \frac{\int_0^1\left[\epsilon\,u' + \frac{\epsilon^2}{1-\epsilon}\mathrm{Fr}\right]r'\,\mathrm{d}r'}{\epsilon_c\left(1 - \frac{2}{p+2}\right)\int_0^1\left[u' + \frac{\epsilon}{1-\epsilon}\mathrm{Fr}\right]r'\,\mathrm{d}r'}, \quad [19]$$

where the Froude number, Fr, is given by

$$\mathrm{Fr} = \frac{V_V}{\sqrt{gD}}. \tag{20}$$

The drift–flux parameter thus depends on four variables, viz. Ga, Fr, ϵ_c and ρ.

DRIFT-FLUX RESULTS FROM THE MODEL

The one-dimensional circulation model described above was used to calculate the drift–flux parameter C_0 for a wide range of column diameters, void distributions, fluid properties and local bubble rise velocities. Table 2 relates void distribution parameters to the average voidage in the column. Figures 7–15 show how C_0 varies with Ga, Fr and void distribution. It is interesting to note that C_0 assumes very high values over most of the operating range, since the velocity profile is dictated entirely by buoyancy effects rather than by a net flow up the column (i.e. wall effects). This is evident in figure 16, which shows one of Hills' void profiles with the sympathetic velocity distribution. This calculated velocity distribution agrees well with the velocity distribution measured by Hills using a Pavlov tube, which is a device that infers fluid velocity from the pressure field around a cylinder. Figure 17 serves to validate the model further with a comparison of predicted centerline velocities with velocities measured by Hills for various gas flowrates.

The model was also used to find C_0 when there is a net flow in the column. In figure 18 the curve for Fr = 0.25 corresponds to air–water upflow in a 100 mm dia pipe with a typical air–water bubble rise velocity of 250 mm/s and with Re based on the net upflow of liquid in the pipe. At high velocities it can be seen that C_0 tends to a value between 1 and 1.5 which is what has been observed

Table 2. Void fractions used in modeling

Center void fraction ϵ_c	Exponent p	Average void fraction $\bar{\epsilon}$
0.1	2	0.050
0.2	2	0.100
0.3	2	0.150
0.1	3	0.060
0.2	3	0.120
0.3	3	0.180
0.1	7	0.078
0.2	7	0.156
0.3	7	0.233

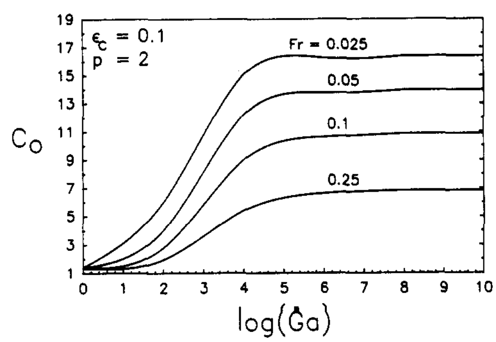

Figure 7. Profile constant C_0 for various Fr and Ga for void distributions given by [1] with $\epsilon_c = 0.1$ and $p = 2$. Fr = 0.25 would correspond to a typical bubble rising in a 100 mm dia column of water. Fr = 0.05 would correspond to a 2.5 m dia column of water. Laboratory scale air-water bubble columns would have Ga = 10^4 to 10^6 and the industrial scale would extend to Ga = 10^8. Ga < 10^3 would occur for viscous systems. The void fraction used here is lower than in an industrial column.

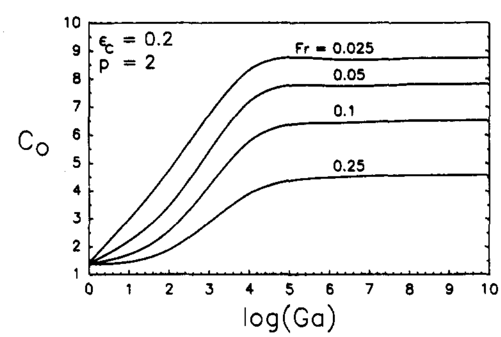

Figure 8. Profile constant C_0 for various Fr and Ga for void distributions given by [1] with $\epsilon_c = 0.2$ and $p = 2$. The comments on Fr and Ga in the legend to figure 7 apply.

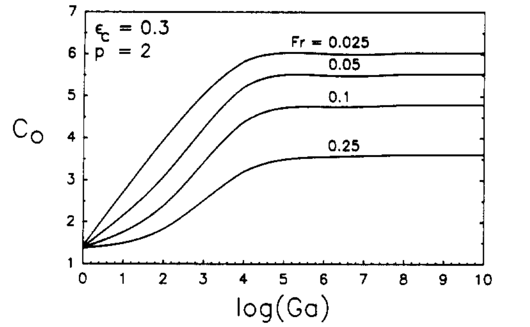

Figure 9. Profile constant C_0 for various Fr and Ga for void distributions given by [1] with $\epsilon_c = 0.3$ and $p = 2$. This would be a realistic void fraction for an industrial column. The comments on Fr and Ga in the legend to figure 7 apply.

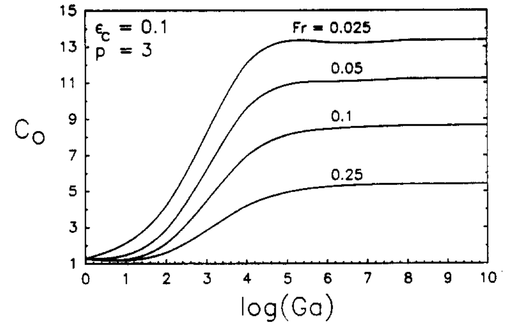

Figure 10. Profile constant C_0 for various Fr and Ga for void distributions given by [1] with $\epsilon_c = 0.1$ and $p = 3$. The comments on Fr and Ga in the legend to figure 7 apply.

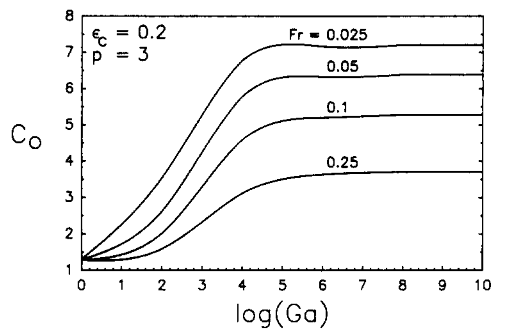

Figure 11. Profile constant C_0 for various Fr and Ga for void distributions given by [1] with $\epsilon_c = 0.2$ and $p = 3$. The comments on Fr and Ga in the legend to figure 7 apply.

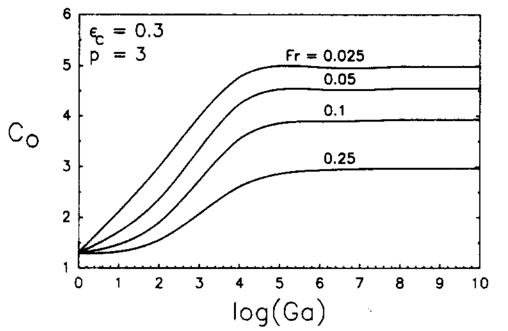

Figure 12. Profile constant C_0 for various Fr and Ga for void distributions given by [1] with $\epsilon_c = 0.3$ and $p = 3$. The comments on Fr and Ga in the legend to figure 7 apply.

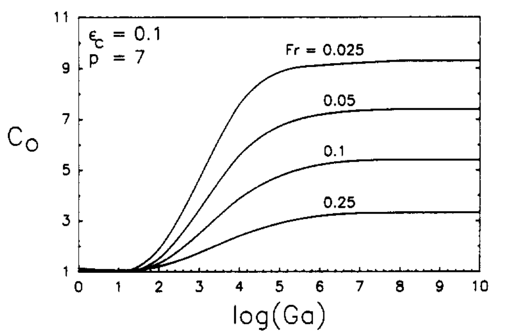

Figure 13. Profile constant C_0 for various Fr and Ga for void distributions given by [1] with $\epsilon_c = 0.1$ and $p = 7$. The comments on Fr and Ga in the legend to figure 7 apply.

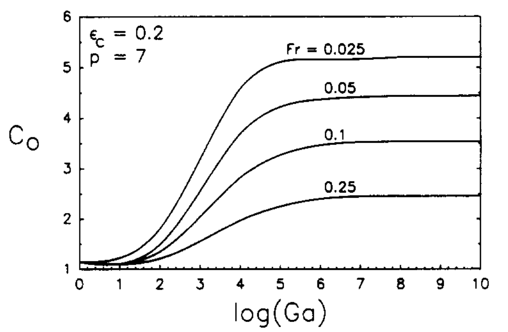

Figure 14. Profile constant C_0 for various Fr and Ga for void distributions given by [1] with $\epsilon_c = 0.2$ and $p = 7$.

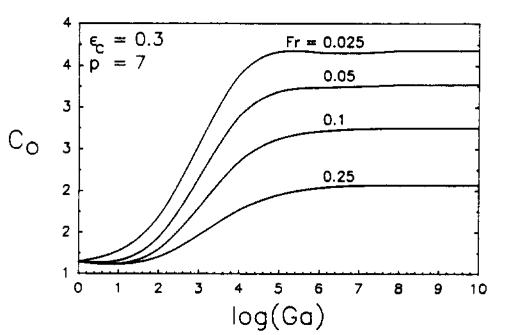

Figure 15. Profile constant C_0 for various Fr and Ga for void distributions given by [1] with $\epsilon_c = 0.3$ and $p = 7$.

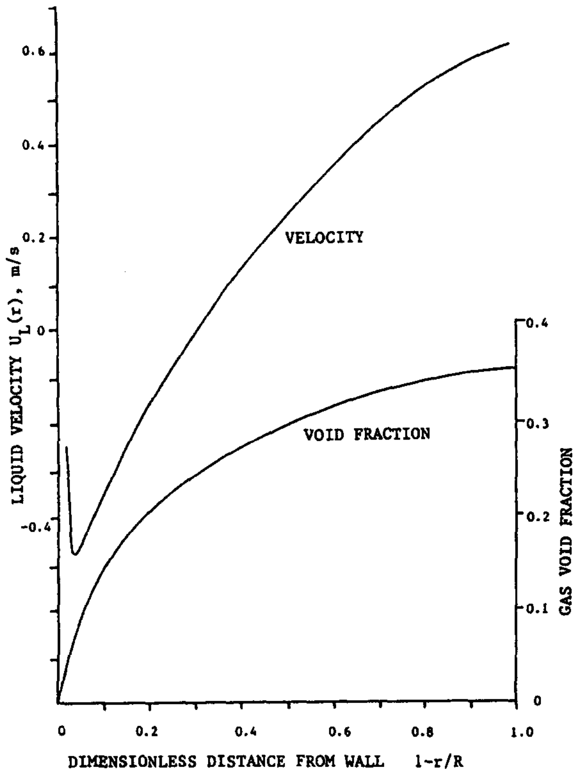

Figure 16. Void profile from the data of Hills (15.2 cm dia column, air superficial velocity 169 mm/s) and the sympathetic liquid velocity profile, found using the method of Clark *et al.* (1987). It is evident that the flow is buoyancy-driven.

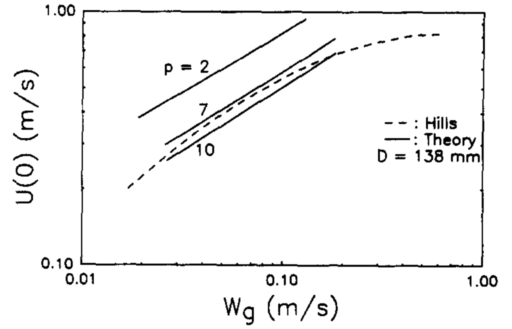

Figure 17. The model was used to predict the centerline liquid velocity in the column when there was no net liquid flow for various gas flowrates and values of the void distribution parameter, p. (Note that ϵ_c can be found given p, W_G and the velocity across the column.) Hills' measured values of centerline velocity are close to the predicted lines for values of $p = 7$ to 10. At very high gas flowrates the mixture properties and behavior will deviate significantly from those of the liquid phase, causing error in the predictions using the present model.

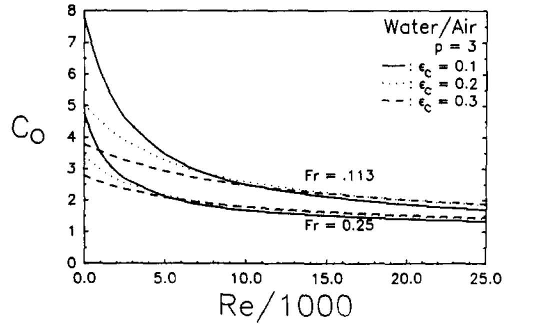

Figure 18. The profile constant, C_0, was calculated for the case where there was a net upflow in the column (represented by the liquid flow $\mathrm{Re} = \rho UD/\mu$) but when buoyancy effects were still significant. $\mathrm{Fr} = 0.25$ corresponds to a bubble rise velocity of 250 mm/s in a 100 mm dia pipe, and $\mathrm{Fr} = 0.113$ for a 500 mm dia pipe.

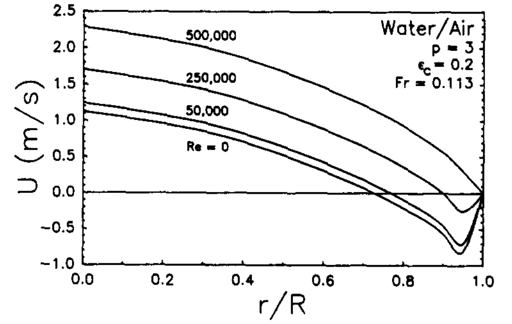

Figure 19. Axial liquid velocity profiles for the case of a 500 mm dia bubble column ($\mathrm{Re} = 0$) and pipe carrying a two-phase upflow ($\mathrm{Re} > 0$), when the void fraction is greatest at the center.

in practice (see table 1). However, at lower velocities buoyancy effects become significant, with C_0 assuming values as high as 3 or 4. This explains the overestimation of void fraction, and hence circulation rate, in some air-lift circulation devices [see comments by Clark & Jones (1987)]. At a larger pipe diameter ($\mathrm{Fr} = 0.113$) buoyancy effects play an even greater role, with a very high centerline velocity existing even at average velocities of 10 m/s. One must conclude the C_0 is highly variable in these circumstances so that a drift–flux model should be used with caution for low velocity or large diameter systems. Figure 19 illustrates some of the predicted velocity profiles which led to the construction of figure 18. The competing buoyancy and wall effects are evident here. Figure 20 yields C_0 when the void fraction is a maximum at the pipe center over a broad range of liquid flow Re values for a 500 mm dia pipe ($\mathrm{Fr} = 0.113$) for both upflow and downflow. A choking condition is evident when the liquid downflow counteracts the upward rise of the bubbles,

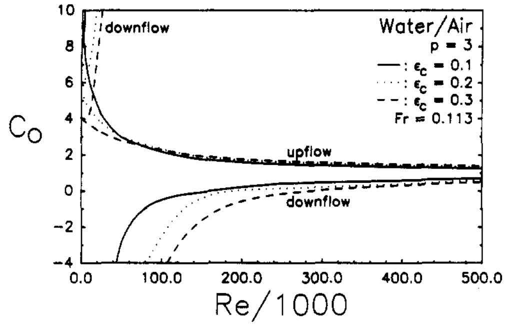

Figure 20. A plot yielding values of C_0, for upflow and downflow, in a 500 mm pipe with the void fraction having a maximum at the pipe center. Note the choking condition for the downflow case, where C_0 assumes very high values: this is when the bubbles cannot rise upward through the downflow, and when the downflow velocity is not strong enough to carry them downward.

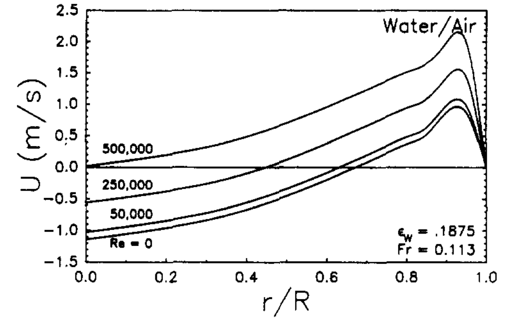

Figure 21. When the bubbles are concentrated in an annular region, buoyancy forces and wall effects are in competition during two-phase upflow. For this case in a 500 mm dia pipe, liquid flow is downward at the center for net upflow Re < 500,000. The void profile used to generate this plot is given in figure 22.

causing a void fraction to be present although $(W_G + W_L) = 0$. Consequently, C_0 assumes very high values.

It is well-documented in the literature (Galaup 1975; Serizawa *et al.* 1975; Nakoryakov *et al.* 1981) that saddle-shaped void profiles can also exist in low void fraction flows, and this is in keeping with the argument presented above for the "inverse" circulation pattern in bubble columns. Figure 21 shows results as velocity profiles from the model for air–water upflow using the annular gas void distribution illustrated in figure 22. Buoyancy effects are so strong for the case of the 500 mm pipe (Fr = 0.113) that the velocity profile remains saddle-shaped (see figure 20) at all credible operating velocities. As a result C_0 remains above unity, despite the fact that the bubbles are concentrated near the wall. However, for a 100 mm pipe (Fr = 0.25), where wall effects are more significant, the computed velocity profile was similar to that in a single-phase flow at higher velocities, so that C_0 was driven to a value below unity.

CONCLUSIONS ON THE DRIFT-FLUX MODEL

(1) In large diameter pipes C_0 will always be greater than unity, assuming very high values at low net flowrates.

(2) In small diameter pipes C_0 will still assume high values due to buoyancy effects at low velocities, but the value of C_0 will depend strongly on the gas void distribution at higher velocities. When the void distribution is saddle-shaped, as occurs at low void fractions, C_0 will be slightly below 1. At higher void fractions, where ϵ is a maximum at the center, C_0 will assume typical values in the range 1.3–1.5.

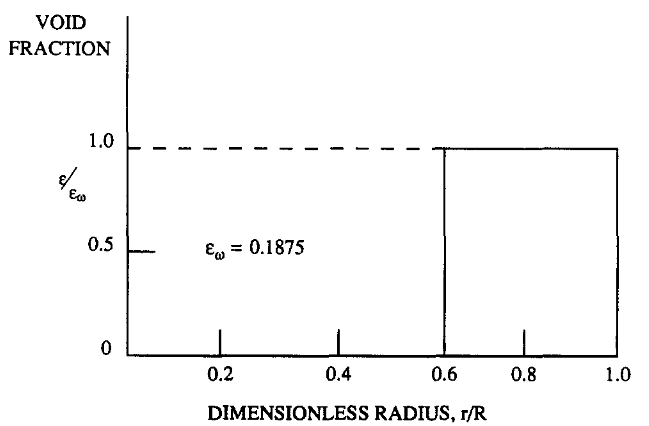

Figure 22. This annular void distribution, intended to imitate saddle-shaped distributions observed by some previous researchers, was used to generate the velocity profiles shown in figure 21.

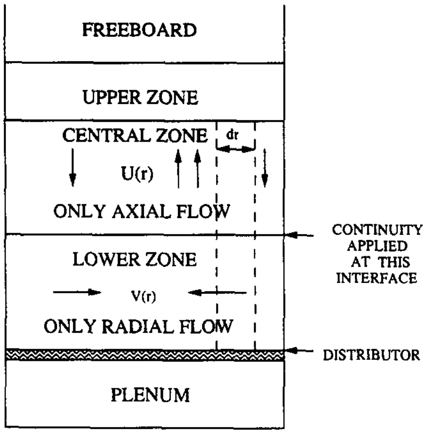

Figure 23. To model radial bubble motion, a two-zone, one-dimensional approach was used. In the central zone, all fluid motion was considered axial. In the lower zone, all liquid motion was considered radial. Bubbles rising vertically through the radial field were moved inward. In this way an uneven void distribution can develop although gas introduction through the distributor may be even.

It can be seen that pipe size, flowrate and void fraction can all influence C_0, so that it is not surprising that many authors have found it necessary to modify drift–flux models to account for these problems. One must conclude that a direct drift–flux approach is not suitable unless the void distribution is known and that buoyancy effects are insignificant.

PREDICTION WITHOUT PRIOR KNOWLEDGE OF THE VOID FRACTION

All of the velocity profiles generated above required prior knowledge of the void profile present in the column, so that *a priori* prediction of circulation is still not facilitated. However, by considering the arguments presented above on the origin of the circulation pattern, and by assuming all bubble motion to be causal (i.e. caused only by gravity and average interphase drag) above the distributor, it should be relatively easy to develop an iterative model for the prediction of circulation in a vessel with even gas distribution, without having to *assume* bubble distributions across the diameter. Select, for the first iteration, an approximate circulation pattern in terms of the velocity distribution across a diameter half way up the column. Then, from continuity considerations, the average radial flux of liquid in the lower half is known at each value of the radius. The transport of bubbles towards the column center by the radial liquid flow in the entrance region can be determined quite accurately, since it is the total radial flux that determines the net bubble movement and the actual radial velocity need not be known as a function of height. The approach yields a gas flux and a voidage distribution half way up the column which can in turn be used to infer a liquid velocity distribution by applying the model described above: the calculation process is then repeated until the predicted velocity distribution agrees with the assumed velocity distribution. In other words we have two models to relate the void distribution and velocity profile. One is the force-balance model, using extensively above. The other involves the "classification" of bubbles which are moved radially as they rise from the distributor to the column center. When these two models agree on the relationship between the void and velocity distributions, we might assume that this is a stable circulation solution. This is discussed in detail below, and an example follows.

Consider the zone in a bubble column just above the distributor plate, and assume that the column contains one large circulation cell, with liquid upflow at the center and downflow at the walls. In this zone there must accordingly be a radially inward flow of liquid. Bubbles rising from the distributor plate will be carried a radial distance inward before they rise to the center section of the column. Let us assume that the lower zone has height h (which is shown to be an arbitrary value) and that the radial velocity components are even over this height, see figure 23. Fluid delivered or removed axially from above to this lower zone will dictate the radial velocity profile. Let $U(r)$ denote the axial velocity in the center zone and $V(r)$ the radial velocity within the lower zone. From conservation of mass, neglecting the volume occupied by bubbles:

$$-2\pi h r V = -\int_r^R 2\pi r U \, dr,$$

which agrees with the fact that V must be zero at the column center and column wall. A bubble rising from the plate with a vertical velocity U_b will spend a time

$$t_z = \frac{h}{U_b}$$

within this zone, and during that time will be swept inwards with a velocity $V(r)$, so that when it leaves the zone it will have moved inwards by a distance given by the integral

$$\int_{t=0}^{t_z} V(r) \, dt.$$

Practically (numerically!) one may trace the path of any bubble through this lower zone, assuming its lateral movement is governed causally by the liquid velocity, to find its position upon leaving the lower zone. For many bubbles, the gas flux $W_{Gb}(r)$ at the base of the lower zone (at the distributor) may be translated into $W_G(r)$ in the central zone. Note that $W_G(r) = \epsilon(r)\,[U_L(r) + V_V]$, in other words, the gas flux is the product of void fraction and gas velocity. This suggests the technique for determining circulation in a bubble column (or a pipe containing low velocity flows) with a knowledge only of distribution performance. The technique involves an assumption of $\epsilon(r)$, followed by calculation of $U(r)$. Hence $V(r)$ may be calculated, and $W_{Gb}(r)$ and $V(r)$, $W_G(r)$ and then $\epsilon(r)$ may be predicted. If this last void distribution is dissimilar from the one originally assumed, a new $\epsilon(r)$ must be assumed and the procedure repeated. Presumably a stable solution results when a given $\epsilon(r)$ [or $W(r)$] will predict the same $\epsilon(r)$ [or $W(r)$], provided that the system can reach that stable condition upon startup. Perturbation studies could also be conducted in this way to assess how robust any particular circulation pattern will be.

An example of this new technique follows, based on the data of Hills. In his paper, data is presented for the void and velocity distributions in a 138 mm dia bubble column operating with

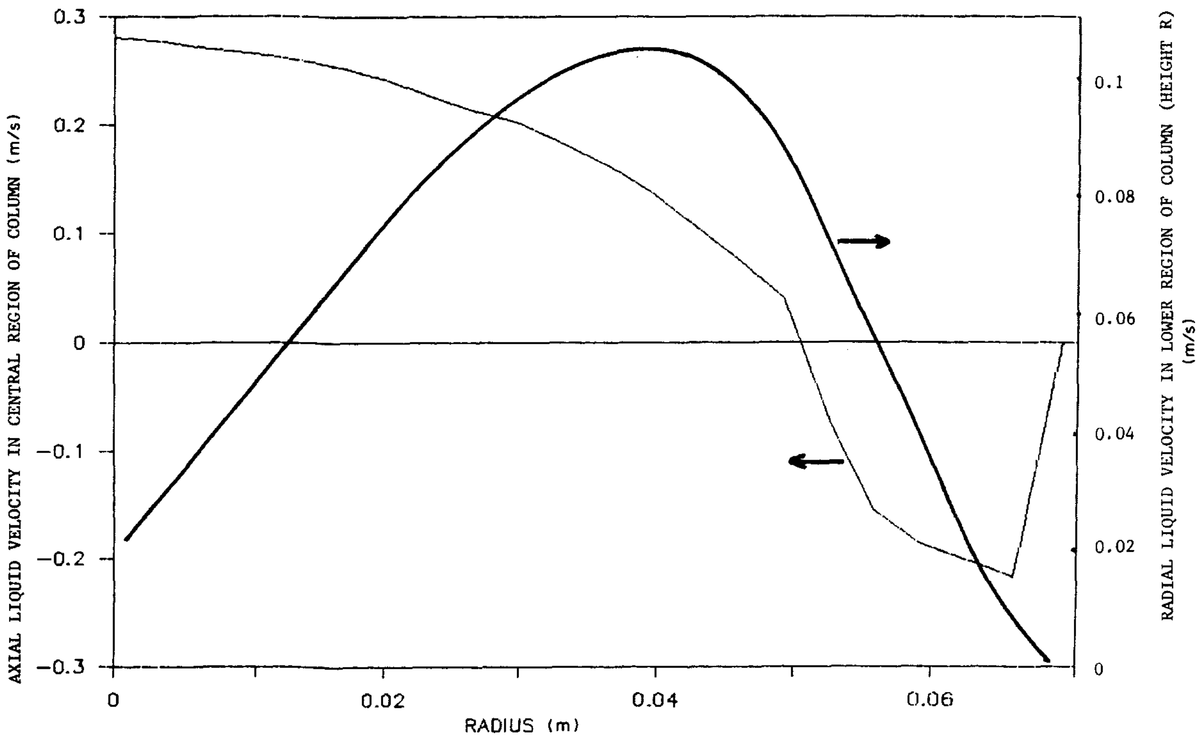

Figure 24. Distribution of radial velocity in the lower zone (V) and axial velocity in the center zone (U), corresponding to Hills' air–water column, with an air superficial velocity of 38 mm/s.

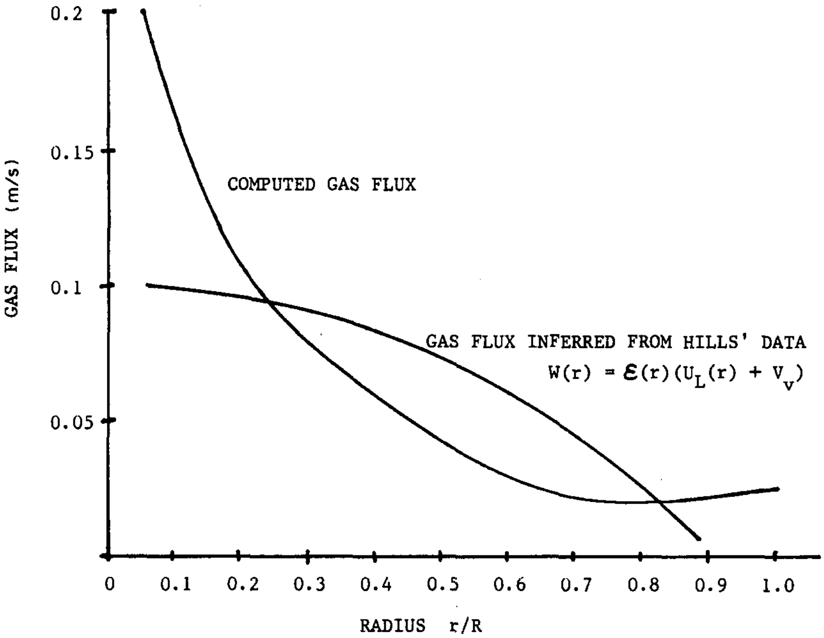

Figure 25. The gas flux, $W(r)$, computed from bubble motion in the lower zone, is compared here with the $W(r)$ found from the product of $\epsilon(r)$ and $(U_L(r) + V_V)$, where data for $\epsilon(r)$ and $U_L(r)$ are given in Hills' paper.

"plate B", which by description should introduce gas evenly over the base of the column. From Hills' figure 11, liquid velocity profiles were obtained for gas fluxes of 169 and 38 mm/s. From Hills' figure 6, data on the void fraction were obtained for the same gas throughputs. A computer program was written in FORTRAN 77 to translate the discrete values of velocity $U(r)$ into radially inward velocities, $V(r)$, in the lower zone above this distributor. This zone was assumed to be one column radius high, but it can be shown readily that this height is arbitrary (a "dummy variable") in this simplified analysis. The program then examined a flux of bubbles rising through this radial flow, being carried inward as they rose. In this way $W_G(r)$ was predicted from $W_{Gb}(r)$, where $W_{Gb}(r)$ was assumed to be an even flux with Hills' plate B.

Figure 24 shows the axial velocities in the center zone and radial velocities in the lower zone for $h = R$ and for the 38 mm/s gas flowrate. Figure 25 shows the computed values of $W(r)$ compared with the values of $W(r)$ $(=\epsilon\ (U_L + V_V))$ found from Hills' paper. While agreement is not excellent, the trends are correct. Errors are ascribed to: (i) inaccuracy in the data; (ii) the discrete and crude approach to finding $V(r)$; (iii) the fact that the volume occupied by bubbles in the lower zone was not considered fully in this simplified model; (iv) the fact that bubble motion might not be entirely causal; and (v) the fact that the distributor plate might not have injected air evenly over the bed cross section. Considerable disagreement toward the column center also arises because errors in volumetric flows are mapped into very small area increments, yielding high errors in computed velocity in this region. Data for the 169 mm/s gas flowrate were in greater error, most likely due to cause (iii) above.

Nevertheless, this is the first "analytic" attempt known to the authors to find turbulent bubble column circulation velocities without prior knowledge of the void profile. Improving this approach will simply lead the researcher to use of a more rigorous fluid computational analysis. It is likely, then, that a two-phase code will be able to predict circulation *a priori*, and research along these lines is currently proceeding at West Virginia University.

Acknowledgements—This paper was prepared with the support of the U.S. Department of Energy, Grant No. DE-FG22-87PC79935. However, any opinions, findings, conclusions or recommendations expressed herein are those of the authors and do not necessarily reflect the views of the DOE. The authors are grateful to John Grosselin for acquiring some of the 15.2 cm column resistance probe data and to Anthony Maeder, a visitor from Monash University, Australia, for FORTRAN programming.

REFERENCES

BORISHANSKIY, V. M., ANDREYEVSKIY, A. A., BYKOV, G. S., ZALETNER, A. F., FOKIN, B. S. & VOLUKHOVA, T. G. 1977 Void fraction and pressure drop in two phase upflow at atmospheric pressure. *Fluid. Mech. Sov. Res.* **6,** 51–61.

CLARK, N. N. & FLEMMER, R. L. C. 1984 On downward two phase flow. *Chem. Engng Sci.* **39,** 170–173.

CLARK, N. N. & FLEMMER, R. L. C. 1985 Predicting the holdup in two phase bubble upflow and downflow using the Zuber and Findlay drift–flux model. *AIChE Jl* **31,** 500–503.

CLARK, N. N. & FLEMMER, R. L. C. 1986 The effect of varying gas voidage and distributions on average holdup in vertical bubble flow. *Int. J. Multiphase Flow* **12,** 299–302.

CLARK, N. N. & JONES, A. G. 1987 On the prediction of liquid circulation in a draft-tube bubble column. *Chem. Engng Sci.* **42,** 378.

CLARK, N. N., FLEMMER, R. L. C. & ATKINSON, C. M. 1987 Turbulent circulation in bubble columns. *AIChE Jl* **33,** 515–518.

GALAUP, J. P. 1975 Ph.D. Thesis, Scientific and Medical Univ. of Grenoble, France.

GOVIER, G. W. & AZIZ, K. 1972 *The Flow of Complex Mixtures in Pipes.* Van Nostrand-Reinhold, New York.

HEWITT, G. F. 1977 Vertical bubble and slug flow. In *Two Phase Flow and Heat Transfer* (Edited by BUTTERWORTH, D. & HEWITT, G. F.). OUP, Oxford.

HILLS, J. H. 1974 Radial non-uniformity of velocity and voidage in a bubble column. *Trans. Instn chem. Engrs* **52,** 1–9.

HILLS, J. H. 1976 The operation of a bubble column at high liquid throughputs—I: gas holdup measurement. *Chem. Engng J.* **12,** 89–99.

HINES, D. A., BAILEY, M., OOSBY, S. C. & ROESLER, F. C. 1975 The ICI deep shaft aeration process. *Instn Chem. Engrs Symp. Ser.* **41,** D1–D10.

IM, C. J., SMITH, L. B. & WOLFE, R. A. 1987 Innovative fine coal drying of UCC Research Corporation and some operation data of commercialized Flotaire column cell in Tanoma coal preparation plant. In *Proc. 4th A. Coal Conf.*, Pittsburgh, Pa, pp. 779–789.

ISHII, M. & GROLMES, M. A. 1978 Constitutive equation for one dimensional drift velocity of dispersed two phase flow. In *Two Phase Transport and Reactor Safety* (Edited by VEZIROGLU, T. N. & KAKAC, S.). Hemisphere, Washington, D.C.

JONES, A. G. 1985 Liquid circulation in a draft-tube bubble column. *Chem. Engng Sci.* **40,** 449–462.

LEVY, S. 1963 Prediction of two phase pressure drop and density distribution from mixing length theory. *ASME Jl Heat Transfer* **85,** 138–152.

LIN, J. S., CHEN, M. M. & CHAO, B. T. 1985 A novel radioactive particle tracking facility for measurement of solids motion in gas fluidized beds. *AIChE Jl* **31,** 465–473.

LORENZI, A. & SOTGIA, G. 1978 Comparative investigation of some characteristic quantities of two phase cocurrent upward and downward flow. In *Two Phase Transport and Reactor Safety* (Edited by VEZIROGLU, T. N. & KAKAC, S.). Hemisphere, Washington, D.C.

MIYAUCHI, T., FURUSAKI, S., MOROOKA, S. & IDEDA, Y. 1981 Transport phenomena and reaction in catalyst beds. In *Advances in Chemical Engineering*, Vol. 11 (Edited by DREW, T. *et al.*), p. 275. Academic Press, New York.

NAKORYAKOV, V. E., KASHINSKY, O. N., BURDUKOV, A. P. & ODNORAL, V. P. 1981 Local characteristics of upward gas–liquid flows. *Int. J. Multiphase Flow* **7,** 63–81.

NASSOS, G. & BANKOFF, S. G. 1967 Slip velocity ratios in an air–water system under steady state and transient conditions. *Chem. Engng Sci.* **22,** 661–668.

NICKLIN, D. J. 1962 Two phase bubble flow. *Chem. Engng Sci.* **17,** 693–702.

ONKEN, V. & WEILAND, P. 1983 Airlift fermentors: construction, behavior and uses. *Adv. biotechnol. Process.* **1,** 67–95.

OTERO, Z., TILTON, J. N. & RUSSELL, T. W. F. 1985 Some observations on flow patterns in tank type systems. *Int. J. Multiphase Flow* **11,** 583–589.

PETRICK, M. & KUDIRKA, A. A. 1966 On the relationship between the phase distribution and relative velocities in two phase flow. *AIChE Proc 3rd Int. Heat Trans. Conf.* **4,** 184–191.

SERIZAWA, A., KATAOKA, I. & MICHIYOSHI, I. 1975 Turbulence structure of air–water bubble flow. *Int. J. Multiphase Flow* **2,** 235–246.

SHIPLEY, D. G. 1984 Two phase flow in large diameter pipes. *Chem. Engng Sci.* **39,** 163–165.

STERN, D., BELL, A. T. & HEINEMANN, H. 1985 Analysis of the design of bubble-column reactors for Fischer–Tropsch synthesis. *Ind. Engng Chem. Process Des. Dev.* **24,** 1213–1219.

SURMA, J. E. 1985 M.S. Thesis, Montana State Univ., Bozeman.

WALLIS, G. B. 1969 *One Dimensional Two Phase Flow*. McGraw-Hill, New York.

ZUBER, N. & FINDLAY, J. A. 1964 General Electric Report GEAP-4592.

ZUBER, N., STAUB, F. W., BIJWAARD, G. & KROEGER, P. G. 1967 General Electric Report GEAP-5417.